PROGESTERONE RECEPTOR IS CONSTITUTIVELY EXPRESSED IN INDUCED PLURIPOTENT STEM CELLS (IPSCs)

Michele Manganelli[1], Elena Laura Mazzoldi[1], Rosalba Monica Ferraro[1], Marta Parigi[1], Seyed Ali Mir Aghel[1], Mattia Bugatti[2], Ginetta Collo[3], Gabriele Stocco[4], William Vermi[2], Luigi Mori[5], Silvia Giliani[1]

[1] "Angelo Nocivelli" Institute for Molecular Medicine, Department of Molecular and Translational Medicine, University of Brescia, Italy, ASST Spedali Civili, Brescia, Italy, 25123, Italy
[2] Department of Molecular and Translational Medicine, University of Brescia, Italy, ASST Spedali Civili, Brescia, 25123, Italy.
[3] Division of Farmacology, Department of Molecular and Translational Medicine, University of Brescia, Brescia, 25123, Italy.
[4] Clinical Department of Medical, Surgical and Health Sciences, University of Trieste, Trieste, I-34127, Italy.
[5] Department of Clinical and Experimental Sciences (DSCS), University of Brescia, Brescia, 25123, Italy.

m.manganelli@unibs.it

Introduction. Induced Pluripotent Stem Cells (iPSCs) are nowadays a common starting point for wide-ranging applications including 3D disease modeling, drug development and regenerative medicine. Physiological processes like homeostasis, cell differentiation and development are tightly regulated by hormones through binding to their receptors of target cells. Considering their pleiotropic effects, it is important to understand their role also during cell differentiation, in particular for those *in vitro* disease models which include steroid hormone cellular response. Here we explored the expression pattern of estrogen receptor (ERα) and progesterone receptor (PR) in four different iPSCs, obtained from CD34+ progenitor cells and skin fibroblasts with four different methods (Table 1) to better define the possible role of steroid-hormone receptors in iPSCs-based cell differentiation modeling.

Table 1. List of iPSCs cell lines used in this study.

iPSCs cell line	Parental cell	Reprogramming Method
Episomal	cord blood-derived CD34+ progenitors	Episomal Vector
BJ	human foreskin fibroblasts	CytoTune-iPS 2.0 Sendai Reprogramming Kit
253-G1	human fibroblasts	Retroviral trasduction
F3	human fibroblasts	Lentiviral trasduction

Results. Expression of ERα and PR mRNA were significantly downregulated in iPSCs as well as fibroblasts compared positive controls (Fig.1-3). Immunofluorescence (IF) staining (Fig.4) detected only the expression of PR protein in all the different iPSCs cell lines, while ERα was not detectable. Blood cells are the most used cell types for reprogramming. In order to explore whether HSPCs would express ERα and PR, we further performed flow cytometry analysis on a G-CSF mobilized-PB control group. We observed (Fig.5) that the ~65% of the total population of iPSCs cells expressed only PR, with 100% fold increase compared to HSPCs and fibroblasts, while ERα was not expressed. Moreover, our results highlighted also that PR expression is dynamic (Fig.6-8): indeed its expression is modulated during mammary-like organoids development, and able to involve PR dowstream target genes expression.

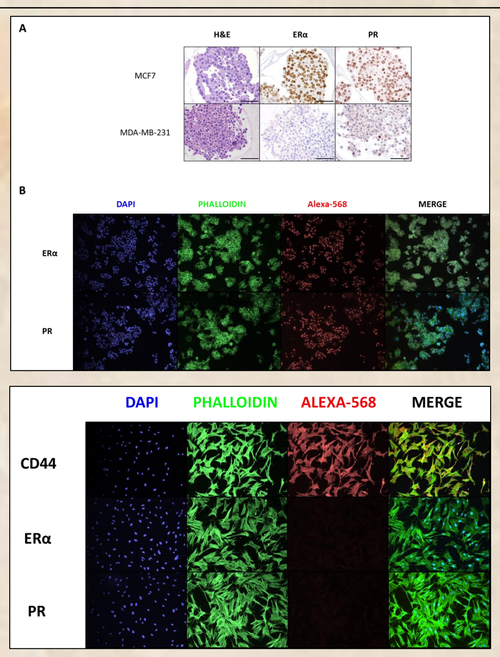

Figure 1. A) H&E and IHC staining for the detection of ERα and PR in mammospheres from MCF7 (ER+, PR+) and MDA-MB-231 (ER-, PR-) cells.
B) IF staining for ER and PR in MCF7 breast cancer cell line positive control.

Figure 2. CD44, ERα and PR in BJ human foreskin fibroblasts. Immunofluorescent (IF) staining. Nuclei were counterstained in blue (DAPI) and cytoskeleton in green (phalloidin-488), while CD44, ERα and PR in red (Alexa-568). Magnification 10X.

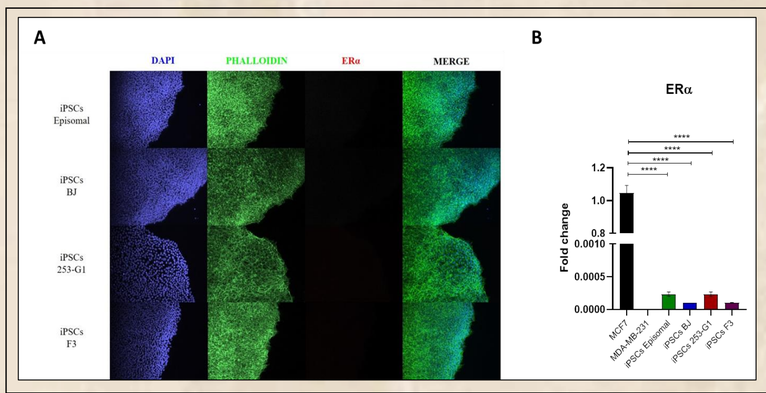

Figure 3. CD44, ERα and PR in BJ human foreskin fibroblasts. A) Immunofluorescent (IF) staining. Nuclei were counterstained in blue (DAPI) and cytoskeleton in green (phalloidin-488), while CD44, ERα and PR in red (Alexa-568). Magnification 10X. B) ERα mRNA in iPSCs cell lines compared to MCF7 positive and MDA-MB-231 negative control.

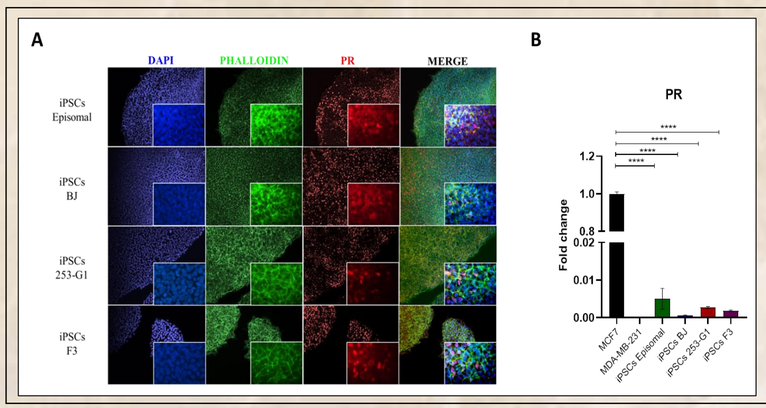

Figure 4. CD44, ERα and PR in BJ human foreskin fibroblasts. A) Immunofluorescent (IF) staining. Nuclei were counterstained in blue (DAPI) and cytoskeleton in green (phalloidin-488), while CD44, ERα and PR in red (Alexa-568). Magnification 10X. B) PR mRNA in iPSCs cell lines compared to MCF7 positive and MDA-MB-231 negative control.

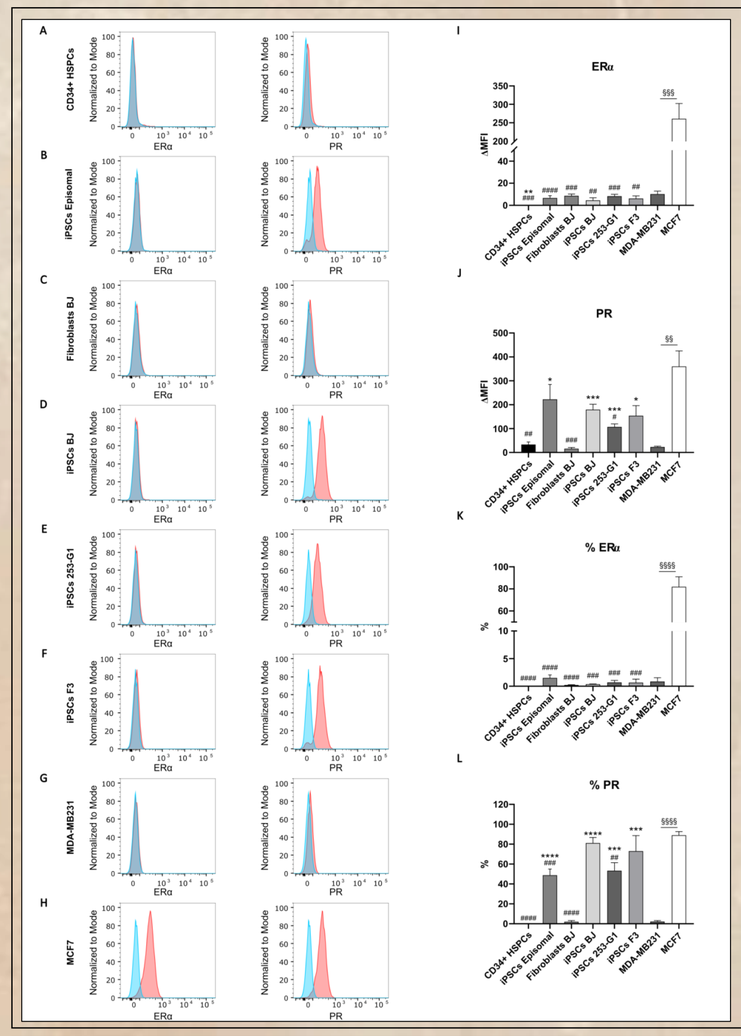

Figure 5. Flow cytometry analysis for the detection of ERα and PR in mobilized-PB, fibroblasts, and iPSCs. A-H: representative images of ERα (left) and PR (right) expression in G-CSF mobilized-PB (gated on CD34+ HSPCs, A), Episomal iPSCs (B), BJ fibroblasts (C), BJ iPSCs (D), 253-G1 iPSCs (E), F3 iPSCs (F), and in MDA-MB231 negative control (G) and MCF7 positive control (H); red = aspecific fluorescence, blue = FITC-labeled target. I-L: Histograms representing either ΔMFI= median fluorescence intensity (I,J) or percentage (K,L) of ERα (I,K) and PR expression (J,L) in G-CSF mobilized-PB (gated on CD34+ HSPCs), Episomal iPSCs, BJ fibroblasts, BJ iPSCs, 253-G1 iPSCs, F3 iPSCs, and in MDA-MB231 negative control and MCF7 positive control. Bars represent the mean ± SEM from at least three independent experiments.*, # p<0.05, **, ##, §§ p<0.01, ***, ###, §§§ p<0.001, ****, ####, §§§§ p<0.0001; * vs MDA-MB231; # vs MCF7; § MDA-MB231 vs MCF7.

Figure 6. Mammary-like organoids generation from iPSCs A) iPSCs colony; B) 1-d mEBs differentiation; C) 10-d mEBs differentiation; D) Mammary-like organoids. Pictures were acquired at 4X (background) and 20X (foreground) magnification respectively.

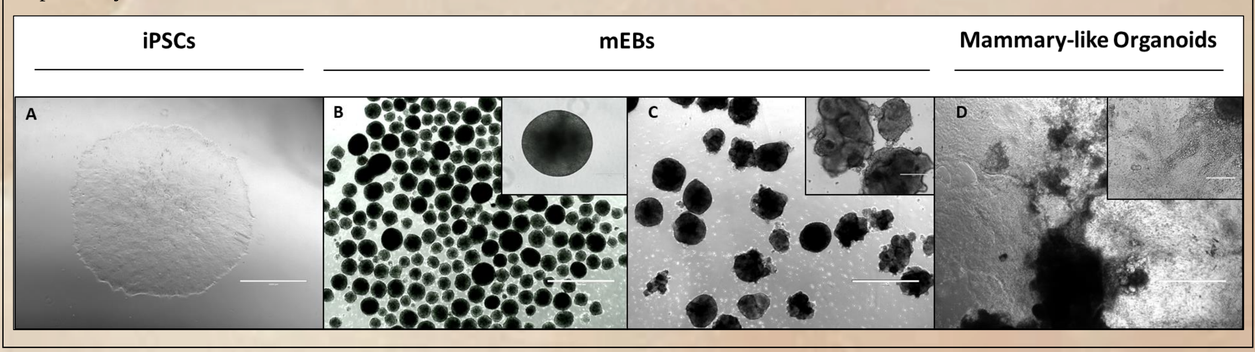

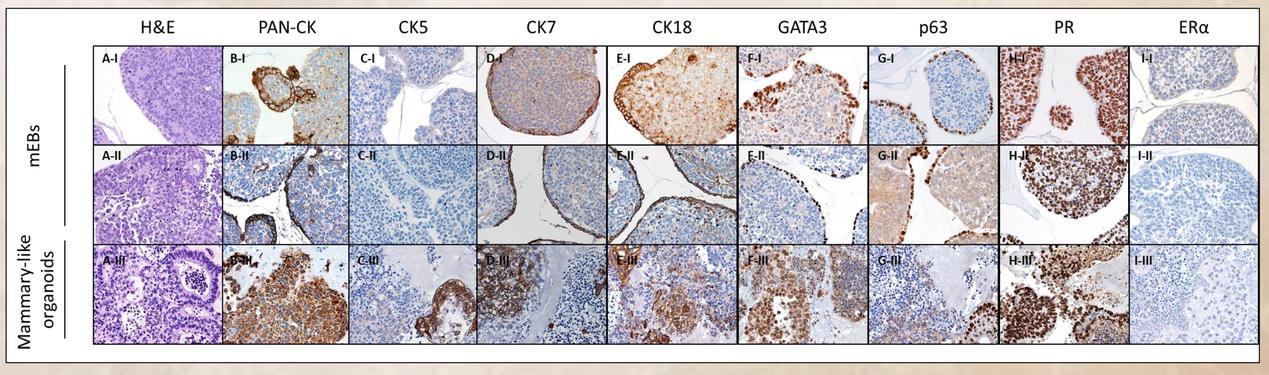

Figure 7. H&E and IHC staining. A) H&E stain; B) PAN-CK; C-D-F) Luminal (CK5/7+ and GATA3+) and E-G) basal cells markers (CK18+ and TP63+); H) PR and I) ERα. Representative images of mEBs obtained from iPSCs Episomal (I); mEBs obtained from iPSCs BJ (II); mammary-like organoids (III) differentiation.

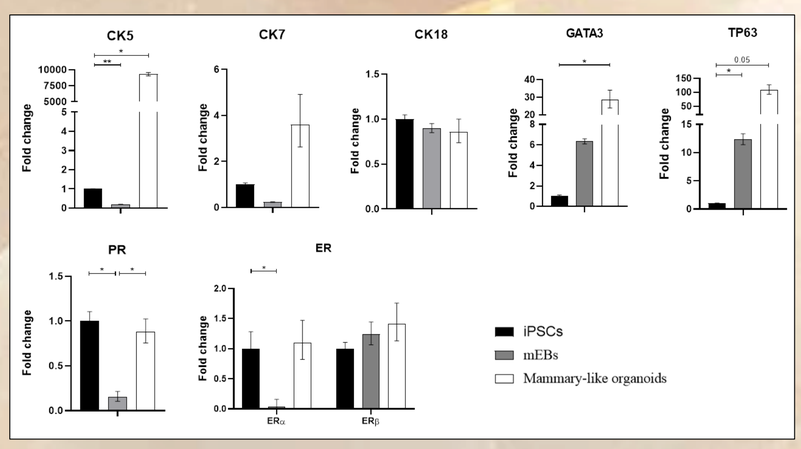

Figure 8. The expression of luminal (*CK5/7* and *GATA3*) and basal markers (*TP63)* indicated the co-existance of several cellular phenotypes during iPSCs differentiation to mammary-like organoid. *PR* expression was significantly reduced in the early stage of differentiation from iPSCs to 10-d mEBs. Accordingly, a similar reduction was observed in *ERα* expression; *ERβ* showed a trend of upregulation during mEBs maturation into mammary-like organoids. Considering PR downstream target genes, *CK5* in the early stage was significantly low expressed in iPSCs and 10-d mEBs compared to mammary-like organoids, where its expression was remakably upregulated during the late stage of differentiation. Regarding *GATA3,* undifferentiated iPSCs expressing elevated levels of *PR*, showed a low expression of *GATA3*. During the early stage of 10d-mEBs differentiation, *PR* and *GATA3* showed opposite trend: the expression of *PR* was reduced while the expression of *GATA3* showed a trend of upregulation, reaching a significant expression during mammary-like organoids differentiation in late stage of 20-d maturation. Subsequently, *PR* expression was restored in 20-d mammary-like organoids to levels similar to that of iPSCs.

Conclusion. Our results collectively demonstrated for the first time that the reprogramming of somatic cells into iPSCs leads to the expression of PR receptor. These findings would improve future research in iPSCs cell-based disease modeling, being a starting point to better comprehend the molecular mechanisms involved in development and cellular response to treatments.